2018

Three-dimensional modeling of nitrate-N transport in vadose zone: Roles of soil heterogeneity and groundwater flux

Simin Akbariyeh
Northern Arizona University, simin.akbarieh@gmail.com

Shannon L. Bartelt-Hunt
University of Nebraska-Lincoln, sbartelt2@unl.edu

Daniel D. Snow
University of Nebraska - Lincoln, dsnow1@unl.edu

Xu Li
University of Nebraska - Lincoln, xuli@unl.edu

Zhenghong Tang
University of Nebraska - Lincoln, ztang2@unl.edu

See next page for additional authors

Three-dimensional modeling of nitrate-N transport in vadose zone: Roles of soil heterogeneity and groundwater flux

Simin Akbariyeh,[1] Shannon Bartelt-Hunt,[2] Daniel Snow,[3] Xu Li,[2] Zhenghong Tang,[4] & Yusong Li[2]

1 Department of Civil Engineering, Construction Management & Environmental Engineering, Northern Arizona University, Flagstaff, AZ, USA
2 Department of Civil Engineering, University of Lincoln-Nebraska, Lincoln, NE, USA
3 School of Natural Resources, University of Nebraska–Lincoln, Lincoln, NE, USA
4 Community and Regional Planning Program, University of Nebraska–Lincoln, Lincoln, NE, USA

Corresponding author — Yusong Li, *email* yli7@unl.edu

Abstract

Contamination of groundwater from nitrogen fertilizers in agricultural lands is an important environmental and water quality management issue. It is well recognized that in agriculturally intensive areas, fertilizers and pesticides may leach through the vadose zone and eventually reach groundwater. While numerical models are commonly used to simulate fate and transport of agricultural contaminants, few models have considered a controlled field work to investigate the influence of soil heterogeneity and groundwater flow on nitrate-N distribution in both root zone and deep vadose zone.

In this work, a numerical model was developed to simulate nitrate-N transport and transformation beneath a center pivot-irrigated corn field on Nebraska Management System Evaluation area over a three-year period. The model was based on a realistic three-dimensional sediment lithology, as well as carefully controlled irrigation and fertilizer application plans. In parallel, a homogeneous soil domain, containing the major sediment type of the site (i.e. sandy loam), was developed to conduct the same water flow and nitrate-N leaching simulations.

Published in *Journal of Contaminant Hydrology* 211 (2018), pp 15–25.
doi 10.1016/j.jconhyd.2018.02.005

Submitted 23 November 2017; revised 16 February 2018; accepted 25 February 2018; published 27 February 2018.

Simulated nitrate-N concentrations were compared with the monitored nitrate-N concentrations in 10 multilevel sampling wells over a three-year period. Although soil heterogeneity was mainly observed from top soil to 3m below the surface, heterogeneity controlled the spatial distribution of nitrate-N concentration. Soil heterogeneity, however, has minimal impact on the total mass of nitrate-N in the domain. In the deeper saturated zone, short-term variations of nitrate-N concentration correlated with the groundwater level fluctuations.

1. Introduction

Nitrate-N leaching due to excessive nitrogen application, irrigation, and inappropriate soil management practices, is a primary cause of groundwater pollution in agricultural regions (Gärdenäs et al., 2005; Zhu et al., 2005; Mitsch and Day, 2006). In areas of intense farming, nitrate-N concentrations in groundwater has been reported to exceed the maximum contaminant level (MCL) of 10 mg L^{-1} for drinking water established by the U.S. Environmental Protection Agency (USEPA) in many areas of the U.S. Elevated nitrate-N concentration in drinking water is harmful to pregnant women and elderly people, and may cause methemoglobinemia in infants under 6 months (Spalding and Exner, 1993; "Water Research Center," 2014).

Numerical modeling is an efficient tool for understanding the physical, chemical and biological processes affecting nitrate-N transport, as well as in predicting and managing nitrate-N pollution (van der Laan et al., 2014). Numerous studies have been published to model the fate and transport of nitrogen in soils, focusing either on nitrogen leaching in the root zone (Nakamura et al., 2004; Skaggs et al., 2004; Gärdenäs et al., 2005; Hanson et al., 2006; Tafteh and Sepaskhah, 2012; Arbat et al., 2013; Deb et al., 2015; Iqbal et al., 2016) or on nitrate-N transport and transformation in the saturated zone (MacQuarrie et al., 2001; Lee et al., 2006). Various models have been applied to simulate soil water and nitrogen dynamics in soils, such as soil-crop model (STICS) (Ledoux et al., 2007; Poch-Massegú et al., 2014; Plaza-bonilla et al., 2015), Root Zone Water Quality Model (RZWQM) (Ma et al., 1998), Agricultural Production Systems SIMulator (APSIM) (Keating et al., 2003), Cropping System Simulation Model (CropSyst) (Stöckle et al., 2003), Soil Water Balance Model (SWB-Sci) (van der Laan et al., 2014), as well as simple models solving water and nitrate-N production functions (Cabon et al., 1991). These modeling efforts have determined the significant impact of various

parameters, such as fertilizer application rate, precipitation pattern, irrigation strategies, and soil types on nitrate- N leaching in soils.

Although these studies generally agree that field non-uniformity widely exists, however, most of them simulated fairly simplified scenarios in the models, assuming either one single soil type (Skaggs et al., 2004; Gärdenäs et al., 2005; Hanson et al., 2006; Deb et al., 2015) or layered soil types (Hassan et al., 2008; Hu et al., 2008; Ramos et al., 2012; Tafteh and Sepaskhah, 2012; Poch-Massegú et al., 2014; Wang et al., 2014; Iqbal et al., 2016; Baram et al., 2017) in a vertical 2D domain. In reality, soil properties varied spatially across the field, which can hardly be captured by point soil samplings. Soil type and grain size distribution strongly influence soil water content distribution. Different soil types typically correspond to different soil organic matter and moisture content, both of which could affect biodegradation rates. Furthermore, horizontal soil texture variation and surface topography could also affect water content distribution and nutrient leaching pathways. For example, surface topography can result in surface water ponding which can influence soil water content distribution as well as soil dissolved oxygen concentration. Heterogeneity may easily influence contaminant biodegradation and leaching rate in the subsurface.

A few three-dimensional (3D) models have been developed to analyze water flow and solute transport in a 3D heterogeneous vadose zone-groundwater system (Russo et al., 2001, 2013; Botros et al., 2012). Russo et al. (2013) clearly demonstrated that simple point 1-D modeling could not accurately simulate the spatial pattern of water content and nitrate concentration produced by rather complicated soil-water-plant-atmosphere flow system. As with many other studies, the model simulated nitrate concentration was not compared against field data (Russo et al., 2013) due to the cost and the need for long-term monitoring. Botros et al. (2012) simulated nitrate transport and storage within a 3-D (6.1m by 6.1m by 15.86 m) heterogeneous vadose zone generated by geostatistical methods and compared the simulated amount of nitrate stored in the vadose zone with field measurements based on seven years of field fertilization data. Their modeling results suggested that numerical based modeling techniques overestimated the measured nitrogen mass in the deeper part of the vadose zone. Clearly, the effect of fate and transport processes, particularly in the deeper part of the vadose zone, is not yet adequately quantified. Most of the available 3D models studied water flow and nitrate-N leaching in relatively small field sites (< 20m in width)

and only focused on the unsaturated part. Typically, a constant pressure head boundary condition was imposed at the bottom of the simulation domain. Potential interactions of groundwater flux on the nitrate-N distribution in the deeper part of the vadose zone were rarely investigated.

In this work, we take advantage of a highly dense data set from a field site in Nebraska Management Systems Evaluation Area (MSEA). The site was relatively well characterized so that a 3D lithologic model can be developed, which provides realistic spatially varied soil properties on the site. For comparison purpose, a homogenous soil domain (sandy-loam soil) was also simulated to compare and analyze the influences of soil heterogeneity. The site has shallow water table providing ideal condition to study the impact of groundwater flux on the distribution of nitrate-N in the deeper part of the vadose zone. Controlled field implementation of irrigation and fertilizer application was conducted in the 1990s and corresponding groundwater level and nitrate-N concentration data were collected. These data include the detailed description of lithology at 70 wells and 11 test holes, annual irrigation water and fertilizer application rates, and changing groundwater levels as well as the nitrate-N concentration at 16 screening depths in 41 multilevel samplers three times a year (Spalding et al., 2001). This rich data set allowed us to compare simulated and measured nitrate-N concentrations in 10 wells on the site for a three-year period strictly following well-controlled irrigation and fertilization strategies. The goal of this work is to better evaluate the impacts of soil heterogeneity, as well as the interactions of groundwater flux, on the transport of nitrate-N in both root zone and vadose zone down to the water table.

2. Site description

The study area was part of the Nebraska MSEA site, which is located within the Central Platte Natural Resources District (CPNRD) of the Platte River Valley (Fig. 1a) (Schepers et al., 1995; Spalding et al., 2001). The 2.27 km^2 MSEA site is in the southeastern Buffalo County, between Shelton and Gibbon, Nebraska, U.S.A. The climate of the study area is continental and temperate, with an annual mean temperature and precipitation of 10 °C and 623 mm, respectively (Mcguire and Kilpatrick, 1998). The MSEA site consists of a buffer area in the upgradient, a component research site, and a demonstration site (Spalding et al., 2001). During

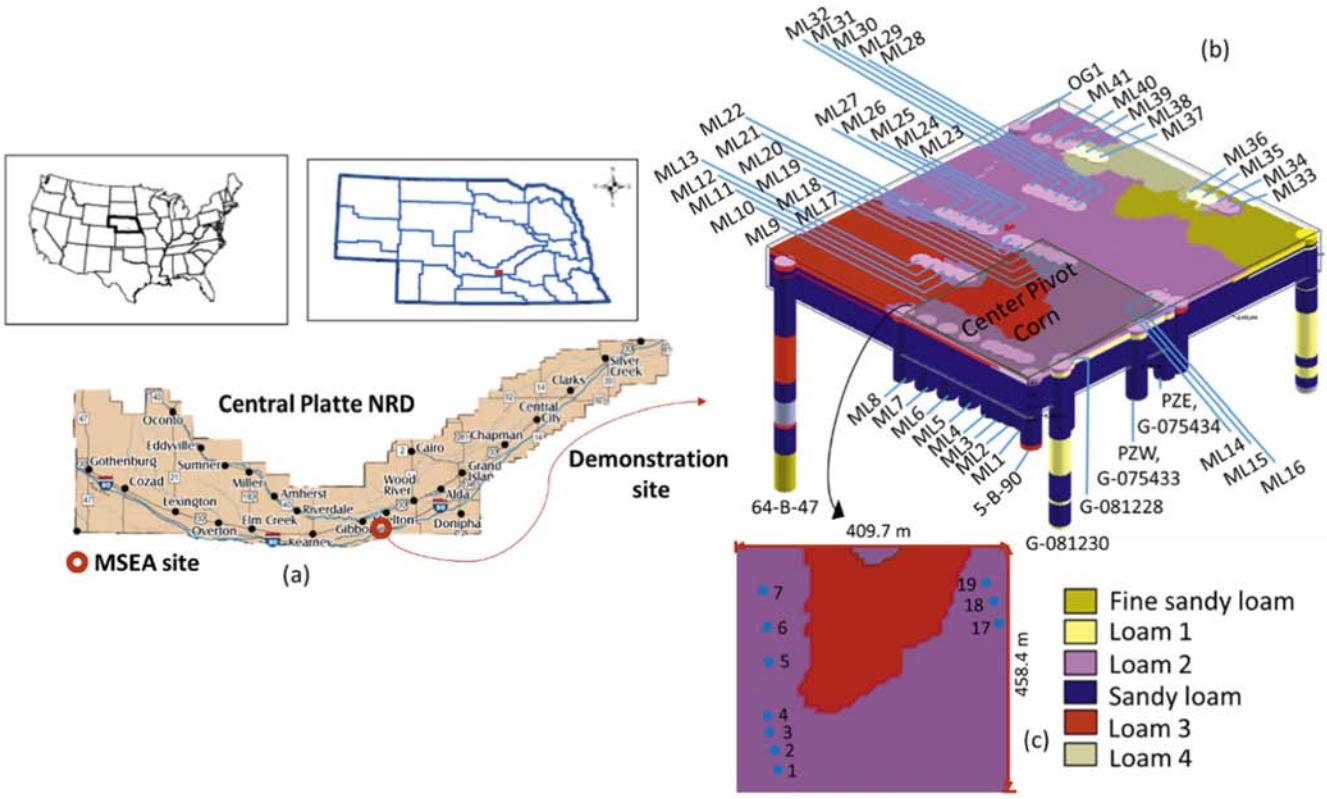

Fig. 1. Case study location and soil lithology model, (a) The location of the MSEA site, (b) 3D lithology model of demonstration site (ML means multilevel samplers), (c) Soil lithology plan view of the simulation domain. The blue points with numbers represent the location of the multilevel samplers.

1993–1995, the demonstration site (914m long and 823m wide) was divided into four fields to implement and evaluate various agriculture management practices: (1) a conventional furrow-irrigated corn field; (2) a surge irrigated corn field (with 60% less water and 31% less N fertilizer application than the conventional field); (3) a center pivot-irrigated corn field (with 66% less water and 37% less N fertilizer application than the conventional field); and (4) a center pivot-irrigated alfalfa (Mcguire and Kilpatrick, 1998; Spalding et al., 2001). During this period, the irrigation and N fertilizer application amounts were controlled and documented. Changing groundwater levels and nitrate-N concentrations were monitored at 41 multilevel samplers (Fig. 1b) in the demonstration site three times a year. Fig. 2 presents the monthly precipitation, irrigation, and average groundwater elevation measured from February 1993 to December 1995.

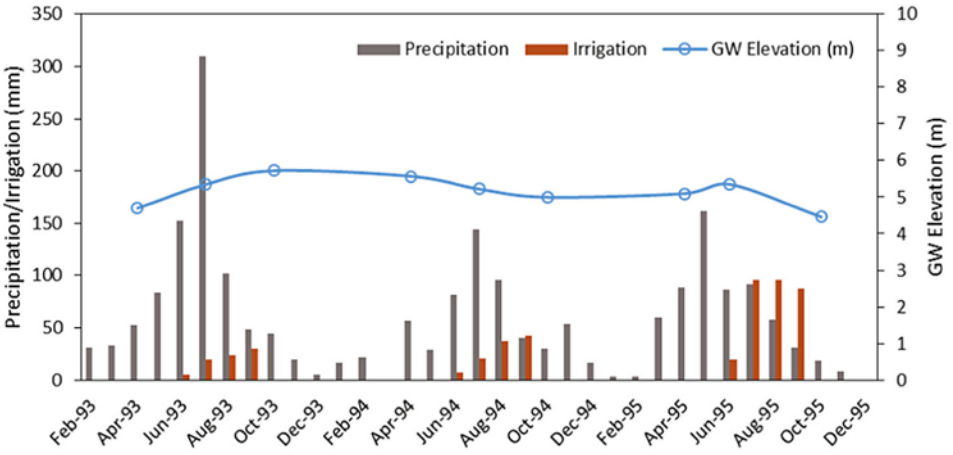

Fig. 2. Monthly plots of precipitation, irrigation, and average groundwater elevation.

With average nitrate-N concentrations between 30 and 32 mg L^{-1} (Mcguire and Kilpatrick, 1998), the shallow and rapidly recharged High Plains alluvial aquifer is mainly used for irrigation. Nitrate-N concentrations in the deeper confined Cenozoic Ogallala Formation aquifer, are <1 mg L^{-1} (Exner and Spalding, 1990; Spalding et al., 2001), however, continued development of this resource will likely lead to impaired water quality as it has in the southernmost extent of this aquifer (McMahon et al., 2006; Chaudhuri and Ale, 2014). In this work, nitrate-N transport modeling was focused on transport beneath the center pivot-irrigated corn field (highlighted in Fig. 1b). Details on N applications in the center pivot-irrigated corn field, including pre-plant, starter, and side-dress (fertilizer applied to the soil on or around the sides of the plant) or fertigation (injected urea-ammonium-nitrate solution into the irrigation water) during 1993–1995 are provided in Table 1.

3. Methods

3.1. Development of a 3-dimentional modeling domain

A three-dimensional (3-D) model of the lithology beneath the demonstration site was created using Rockworks15 ("RockWare, Inc.", 2016), a software widely used for subsurface data visualization. Rockworks interpolated the historically available well logging information (University of Nebraska–Lincoln, 2000) at different locations, including coordinates,

Table 1. Modeling parameters.

Soil Properties

			van Genuchten-Mualem Parameters					
*Soil type** *(from soil samples)*	*Organic matter (%)*	*Bulk density*[1] *(kg m^{-3})*	θ_r	θ_s	α [m^{-1}]	n	K_s[md^{-1}]	l
Loam 1	1.8	1300	0.049	0.402	0.7	1.58	0.25	0.5
Loam 2	1.4	1300	0.051	0.396	0.96	1.51	0.16	0.5
Sandy loam	0.3	1650	0.034	0.390	3.59	1.43	0.56	0.5
Loam 3	1.2	1300	0.058	0.398	1.29	1.46	0.12	0.5
Longitudinal dispersivity, D_L [m]	1.16	Transverse dispersivity, D_T [m]					0.2	

Modeling parameters

Root dist. parameters [m]		*Solute transport (nitrate-N)*	
Max. root depth	1	Urea to ammonium 1st order rate constant, μ [d^{-1}]	0.38
Max. root intensity depth	0.3	Ammonium to nitrate 1st order rate constant, μ [d^{-1}]	0.2
		Ammonium adsorption coefficient, K_d [m^3 kg^{-1}]	3.5×10^{-3}

Field data

Nitrogen application[2] *[kg ha^{-1}]*

	Residual	*Irrigation*	*Starter+Side-dress/Fertigation*	*Pre-plant*	*Irrigation [mm]*
1993	21	24	90	68	79
1994	68	31	62	98	107
1995	83	95	188	–	307

* The analysis of the soil samples collected from the center pivot-irrigated corn field demonstrated different soil types than the labeled soil categories on bore logs.

1. http://www.agriinfo.in/?page=topic&superid=4&topicid=271

2. Spalding et al., 2001.

surface elevations, total depths as well as lithology, and then generated a surface topography map and a continuous lithology model (Fig. 1b). Rockworks uses advanced geostatistical methods to perform three-dimensional interpolation of the borehole data. The horizontal lithoblending method (with both randomize blending and interpolate outliners options) was applied for this case to create the lithology solid model. The numerical modeling domain covers the center pivot-irrigated corn field, which is 458m long and 410m wide (Fig. 1c). In order to further confirm the actual soil properties, soil samples were collected on the site from the location of the wells. Soil particle size distribution analysis was conducted, providing the percentage of silt, sand, and clay. Soil categories from historical well log information were more closely matched

with recent field measurements and previously-described soil categories were corrected based on the measurements, and hydrological parameters were estimated using measured soil properties (Table 1). According to the soil particle size distribution analysis, the deeper part of the simulation domain mainly consists of homogenous sandy loam, while closer to the ground surface it contains four different types of loam (Fig. 1b).

A lithology model of the center pivot-irrigated corn field was then imported into Hydrus (2D/3D) (Šimůnek et al., 2016). Based on the lithology index of each node in the lithology model (in Rockworks), an index was assigned to the closest node in the Hydrus model. Corresponding soil type labels were then applied to all nodes based on the assigned index. Covering the unsaturated zone and about half of the shallow groundwater thickness, the depth of the modeling domain varied between 8.99 and 9.48m due to the uneven surface topography. In the Hydrus 3D model, the horizontal mesh element size was 10 m, and 20 vertical mesh layers were defined with gradually increased layer density from the surface to the bottom boundary.

3.2. Governing equations for water flow

Richards equation was solved to simulate isotropic water flow:

$$\frac{\partial \theta}{\partial t} = \frac{\partial}{\partial x}\left[K(h)\frac{\partial h}{\partial x}\right] + \frac{\partial}{\partial y}\left[K(h)\frac{\partial h}{\partial y}\right] + \frac{\partial}{\partial z}\left[K(h)\frac{\partial h}{\partial z}\right] + \frac{\partial K(h)}{\partial z} - S \qquad (1)$$

where, θ is the volumetric water content [$L^3 L^{-3}$], h is the pressure head [L], t is time [T], x, y, and z are the spatial coordinates [L], S is a sink term [T^{-1}] accounting for root water uptake, $K(h)$ is the unsaturated hydraulic conductivity [$L\ T^{-1}$] which is the product of relative hydraulic conductivity, K_r, and the saturated hydraulic conductivity K_s [$L\ T^{-1}$]. Van Genuchten-Mualem (Mualem, 1976; van Genuchten, 1980) relationships were used to describe the relationship between unsaturated hydraulic conductivity and water saturation and pressure head:

$$K(h) = K_s S_e^{l}\left[1 - \left(1 - S_e^{1/m}\right)^{m}\right]^2 \qquad (2)$$

$$S_e = \frac{\theta(h) - \theta_r}{\theta_s - \theta_r} = \left[1 + \left|\alpha h\right|^{n}\right]^{-m} \qquad (3)$$

where, S_e is effective water saturation [−], θ_r and θ_s are the residual and saturated water content [−], respectively, α [L^{-1}], m, and n [−] are soil type dependent empirical parameters where $m = 1 - 1/n$ and l is tortuosity coefficient [−] which is assumed to be 0.5 (Mualem, 1976). The values of these parameters (i.e. θ_s, θ_r, K_s, and empirical parameters) were estimated based on Rosetta (Schaap et al., 2001), a pedotransfer function model, and the measurements of the soil and sediment samples collected from MSEA site (Table 1). When the n parameter for soil samples is smaller than 2 and a considerable portion of the model domain is saturated, hydraulic conductivity values based on the van Genuchten-Mualem model can be very sensitive to the shape of the soil water retention curve near saturation. For the purpose of confirmation, the model was also simulated using a modified van Genuchten model with an entry pressure specified (Ippisch et al., 2006), which provided< 1.5% differences of the water pressure and nitrate-N concentration values across the simulation domain.

The sink term, S, in eq. (1) represents the plant root water uptake which was defined based on a water stress response function (Feddes et al., 1978):

$$S(h) = \alpha\,(h) S_p\,, \qquad S = \frac{1}{L_x L_y L_z}\; S_t T_p \tag{4}$$

where, α(h) is a dimensionless function of the soil water pressure head ($0 \le \alpha \le 1$) [−], and S_p is the potential water uptake rate [T^{-1}], T_p is the potential transpiration rate [$L\ T^{-1}$], L_z is the depth of the root zone [L] which is considered to be 1m ("Soil and Health Library," 2016), L_x and L_y are the length and width of the root zone [L] which are assumed to be 0.3m for each crop, and S_t is the soil surface associated with transpiration [L_2] (Šimůnek et al., 2016). Water uptake is assumed to be zero when water content is close to saturation or pressure head is below the wilting point (Feddes et al., 1978).

3.3. Governing equations for solute transport

In the simulation, a mixture of urea-ammonium-nitrate was applied onto the center pivot-irrigated corn field as a fertilizer. The transport of the chemical species in a variably saturated porous media with a sequential

first-order decay chain can be simulated as: (Šimůnek et al., 2016)

$$\frac{\partial \theta c}{\partial t} + \rho \frac{\partial_{Sk}}{\partial t} = \frac{\partial}{\partial x_i}\left(\theta D_{ij,k} \frac{\partial c_k}{\partial x_j}\right) - \frac{\partial q_i c_k}{\partial x_i} - \mu_{w,k}\theta c_k - \mu_{s,k}\rho s_k + \mu_{w,k-1}\theta c_{k-1} + \mu_{s,k-1}\rho s_{k-1} - Sc_{r,k}\ , \quad k\ \varepsilon\ (2, n_s) \tag{5}$$

where, c and s are liquid phase [M L^{-3}] and solid phase [MM^{-1}] concentrations, respectively, ρ is the soil bulk density [M L^{-3}], x is spatial coordinates [L] (i=x, y, z), D_{ij} is the effective dispersion coefficient tensor [L^2 T^{-1}] for the liquid phase estimated based on a scale-dependent empirical method proposed by (Neuman, 1990) (Table 1), q is the volumetric flux density [L T^{-1}], μ_w *and* μ_s are first-order decay rate constants in liquid and solid phases [T^{-1}], respectively, which are the connections between individual chain species, S is the sink term [L^3 L^{-3} T^{-1}] in the water flow equation (eq. 1), c_r is the concentration of the N specie in the root zone [M L^{-3}], subscript k is the kth chain number, and n_s is the number of species in the reaction chain.

Sequential first-order decay reactions (Tillotson, 1980), were considered for the transformation of nitrogen in this study. Correspondingly, c_1 is urea, c_2 is ammonium, and c_3 is nitrate-N. Urea ($(NH_2)_2CO$) was assumed to be rapidly hydrolyzed to ammonium (NH_4^+) in water by heterotrophic bacteria and then nitrified to nitrite (NO_2^-) and nitrate (NO_3^-) by autotrophic bacteria. Because the transformation from nitrite to nitrate is much faster than the nitrification of ammonium to nitrite (Hanson et al., 2006), nitrite species was neglected in the simulation. Denitrification was not considered at this stage of modeling because previous isotope analysis of nitrate-N indicated that denitrification was not an important process affecting ground water nitrate-N at this location (Martin et al., 1995; Spalding et al., 2001). Nitrate-N and urea concentrations were defined in liquid phase only, while the sorption of ammonium onto soil was also considered. The first order reaction coefficient (μ_w) for urea to ammonium and for ammonium to nitrate were defined as 0.38 (1/day) and 0.2 (1/day), respectively, based on reported values in literature (Misra et al., 1974; Selim and Iskandar, 1981; Lotse et al., 1992; Ling and El-Kadi, 1998; Hanson et al., 2006; Jansson and Karlberg, 2010). A linear sorption isotherm model was used to simulate the adsorption of ammonium to solid phase (s_k). K_d, is the distribution coefficient [L^3M^{-1}] which was determined to be 3.5×10^{-3} m^3 kg^{-1} according to the literature (Lotse et al., 1992; Ling and El-Kadi, 1998; Hanson et al., 2006).

Root uptake of nutrients, in forms of urea, ammonium, and nitrate-N, was simulated by multiplying root water uptake S to the dissolved nutrient concentration ($c_{r,k}$), when $c_{r,k}$ is lower than the maximum root solute concentration c_{max}, or by multiplying S to c_{max} if c is larger than $c_{max,}$. c_{max} was estimated as 0.033 kg m^{-3} nitrogen based on the maximum corn grain yield (~14 Mg ha^{-1}) in the demonstration site (Spalding et al., 2001) and the reported nitrogen requirements of corn ("Nitrogen Efficiency", 2016).

3.4. Initial conditions

The initial pressure head at the bottom of the domain was obtained by interpolating the groundwater level on April 1st, 1993 in multilevel samplers in the center pivot-irrigated corn field. The soil profile was considered to be in hydrostatic equilibrium with the local groundwater level and initial pressure head was obtained by linear interpolation of the top (surface) and bottom (bottom layer of the domain) pressure head values. The initial urea and ammonium concentration in the subsurface were considered as zero (no N carryover). The groundwater nitrate-N concentrations measured on April 1st, 1993 were used as the initial nitrate-N concentration in the saturated zone. In the previous field studies, the residual nitrate-N concentration was measured at each multilevel sampler to a depth of 1.2m in each spring before planting (Klocke et al., 1999). The initial nitrate-N concentration of the domain was obtained by interpolating the measured nitrate-N concentration at different screening depths of each multilevel sampler.

3.5. Boundary conditions

An atmospheric boundary condition was implemented at the surface, which required daily precipitation, irrigation and potential evaporation and transpiration rates. Daily precipitation and potential evapotranspiration data (ET for reference crop, alfalfa from 1993 to 1996) were collected from Shelton weather station ("High Plains Regional Climate Center website", 2016) located about 2.8 km south from MSEA site, which is the closest weather station to the study site. The total yearly irrigation amount (Table 1) was applied daily, on days with zero precipitation during the irrigation season (late June to end of September) (Spalding et al., 2001). The reference ET (adopted from Shelton weather station)

was calculated using the Penman-Monteith method. To separate the potential evaporation and potential transpiration, Bear's law was applied (Šimůnek et al., 2016). Surface cover fraction (SCF) was first calculated from leaf area index (LAI). LAI was obtained based on a report from the US-Ne2 site, which is another University of Nebraska research field with irrigated maize and soybean rotation ("AmeriFlux Site and Data Exploration System", 2016). A variable pressure head boundary condition was implemented at the bottom boundary to consider the groundwater elevation fluctuations during the simulation. The daily rate of groundwater elevation change was obtained by linearly interpolating the groundwater level measurements at 14 different times after April 1st, 1993. For both water flow and solute transport, zero flux boundary condition was applied at the vertical boundaries, which is the HYDRUS 3D default boundary condition and assumes that water and solute influx through side boundaries was compensated by outflux (symmetry domain) (Skaggs et al., 2004; Gärdenäs et al., 2005; Iqbal et al., 2016).

For solute transport, the third type (Cauchy type) concentration flux boundary condition was specified along the surface boundary to prescribe nitrogen application. Nitrogen was applied at various times during 1993–1995 known as pre-plant-N, starter-N, side-dress/fertigation-N and irrigation-N (Table 1) (Spalding et al., 2001). Starter-N and side-dress/fertigation-N were assumed to be added during the irrigation season (late June to end of September (Spalding et al., 2001)) and were mixed with nitrate-N in irrigation water (30 mg L^{-1}). Pre-plant-N was assumed to be applied in late March (Spalding et al., 2001). Concentration flux boundary condition (third type) was also applied at the bottom of the domain to prescribe a concentration flux defined by the groundwater nitrate-N concentration (30 mg L^{-1}) and groundwater flux along the bottom boundary.

4. Results and discussion

4.1. Comparison between modeling results and field *data*

Fig. 3 shows the comparison of simulated and measured vertical profiles of nitrate-N concentration on October 1st and April 1st of 1993 to 1995 in ML1, ML5, ML7, and ML19. ML1, ML5, and ML7 are in the western part of the field and ML19 is in the eastern part of the field (Fig. 1).

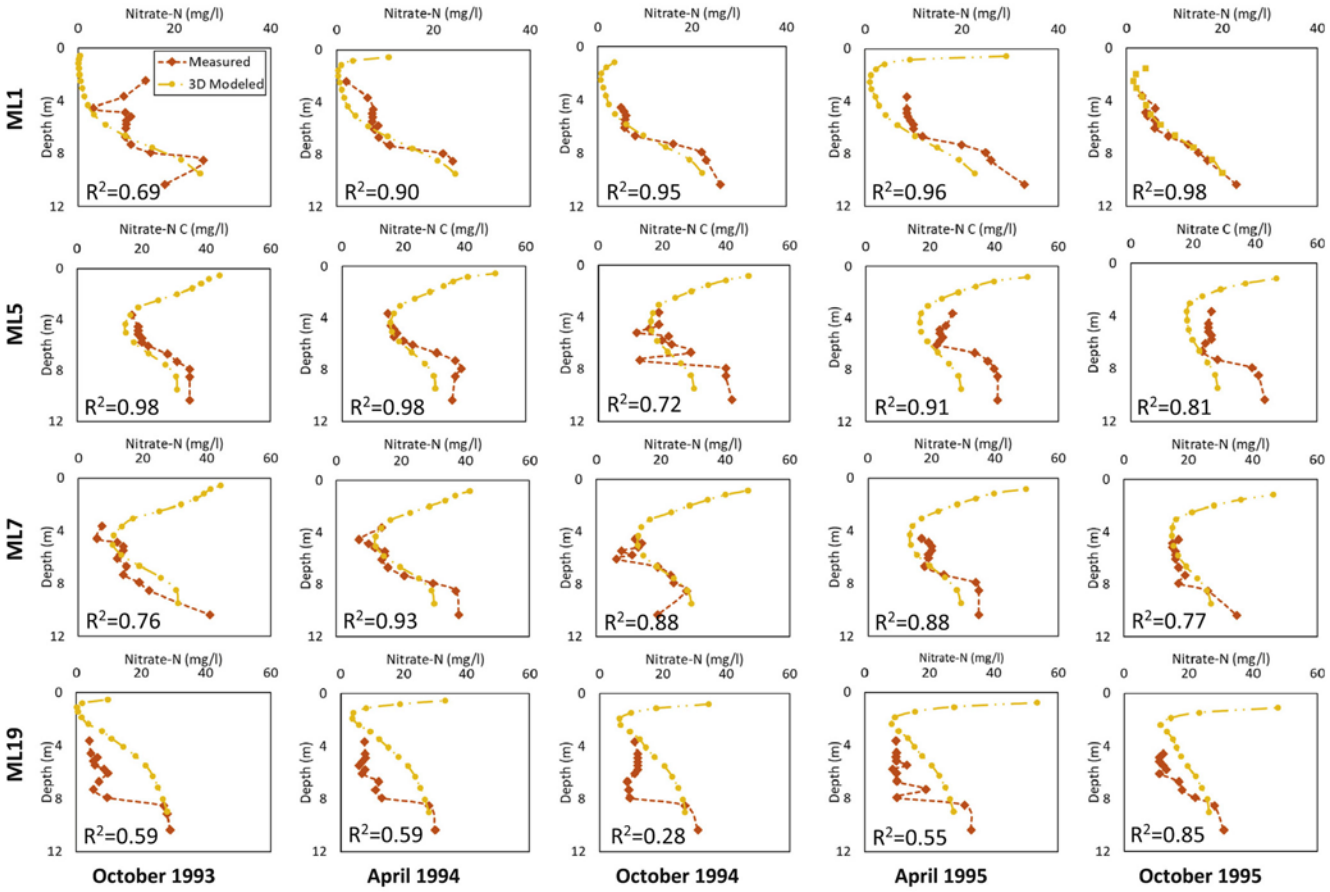

Fig. 3. Vertical profiles of nitrate-N concentration measured by four multilevel samplers from October 1993 to October 1995. Values of coefficient of determination are shown on each concentration profile.

The nitrate-N concentration was mostly high near the ground surface due to the application of fertilizer. Applied nitrate-N rapidly infiltrated into the subsurface due to both subsequent precipitation and irrigation, which was then sharply reduced from about 20–40 mg L^{-1} on the surface to <10 mg L^{-1} at a depth of about 2–4m from the surface. Changing groundwater nitrate-N concentration measurements were based on multilevel samplers, however no comparable data was available to compare with the simulated nitrate-N concentration in the unsaturated zone. In the saturated zone (about 3m below the ground), the measured nitrate-N concentrations in three multilevel sampler close to the western boundary of the field (i.e. ML1, ML5, and ML7) were closely matched with the simulated results at different screening depths across the whole investigation period, with the coefficient of determination (R^2) ranged

between 0.69 and 0.98. The good agreement indicated that the mathematical model has accounted for the important processes controlling nitrate-N transport in the area including soil heterogeneity. Despite good agreement for ML1, 5, and 7, simulated nitrate-N concentrations in a multilevel sampler close to the eastern boundary of the domain (ML19) were about 1.2 to 3 times higher than the measured values (R^2 between 0.28 and 0.85). From October 1993 to October 1995, the nitrate-N concentration was measured eight times per year in 10 multilevel samplers (Fig. 1c) for evaluation of sampling bias each at five to seven screening depths (a total of 509 field measurements). The overall coefficient of determination for all 509 field measurements is 0.6, with distinctly higher R^2 values in the western part of the domain (ML1-7, average R^2 of 0.87), and much lower R^2 values in the eastern part of the domain (ML17-19, average R^2 of 0.57). Possible reasons for this discrepancy could be due to preferential flow paths or local denitrification process in the unsaturated zone. For instance, there might be preferential or non-uniform flow paths in this region (i.e. 2 to 8m below the ground surface), which facilitated nitrate-N movement toward the groundwater and reduced the concentration. Based on uniform nitrogen isotope composition, denitrification process was assumed to be limited in the groundwater because dissolved organic carbon (DOC) concentrations were too low (Spalding et al., 2001). Based on the N_2/Ar ratios measurements on this site, Martin et al. (1995) also demonstrated that N_2 was not in excess of air-saturated water values in most of the sampled cluster wells, indicating that denitrification was very limited in the shallow groundwater. However, this does not rule out the possibility of denitrification in local areas, particularly in stagnant zones of water flow. In a similar nitrate-N transport study by Botros et al. (2012), numerical models were found to overestimate the field measurement nitrate-N mass, which was partially attributed to spatially variable denitrification. More field data and measurements are needed to incorporate a spatially variable denitrification process, despite the incorporated soil heterogeneity in the model. In this simulation, all parameters were either direct field measurements or estimated from measured soil properties. No parameter fitting was conducted. Although the discrepancies exist for some parts of the domain, the overall agreement between the modeling and field measured data in most cases, on a realistic field site for a 3-year simulation period, indicates that the model captured most important processes that control the transport of nitrate-N in the area.

4.2. Impact of groundwater fluctuation on nitrate-N in the domain

Different from commonly reported profiles in literature where nitrate-N concentration continuously decreased with increasing depth, after reaching a minimum, the nitrate-N concentration gradually increased in the deeper part of the aquifer and reached a value of about 30 mg L^{-1} at the bottom of the modeling domain. We hypothesize that the higher concentration of nitrate-N in the deeper part of the domain was due to the influence of groundwater flux. Groundwater in this area was contaminated with an average nitrate-N concentration of about 32 mg L^{-1}, attributed to over 30 years of excess irrigation water and fertilizer application in furrow irrigated corn up-gradient of the site (Spalding et al., 2001). Nitrate-N in the groundwater was brought into the domain when groundwater elevation was increased. Previous studies in the same field also hypothesized that induced flux led to seasonal changes of nitrate-N concentration (Lasserre et al., 1999; Spalding et al., 2001; Stigter et al., 2011), which, however, was based on the average value of nitrate-N concentration at several locations beneath the whole center-pivot irrigated corn field. In this work, a variable pressure head boundary condition was implemented at the bottom boundary to consider the groundwater elevation fluctuations during the simulation period. To testify the role of groundwater elevation fluctuation on the distribution of nitrate-N in the deeper part of the modeling zone, we conducted another simulation by applying a constant pressure head boundary condition at the bottom of the domain (**Fig. 4**). As illustrated in Fig. 4, a constant pressure boundary condition predicted a very low nitrate-N concentration

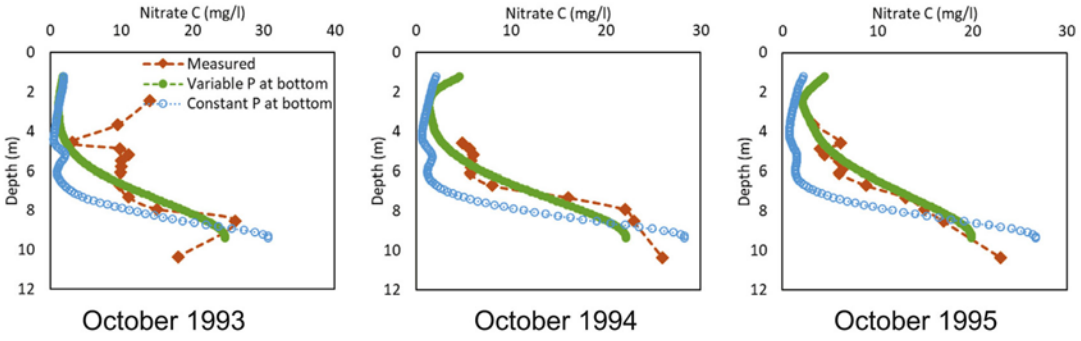

Fig. 4. Comparison between the simulated NO_3-N concentrations in ML1 with variable pressure head (groundwater elevation) boundary condition and a constant pressure head boundary condition at the bottom of the domain.

down to about 6m from the ground and then a sharp increase close to the bottom boundary. Furthermore, the nitrate-N concentration profile predicted by a constant pressure head boundary condition does not change over time. A variable pressure head boundary condition was able to produce the gradual increase of the nitrate-N concentration with depth as well as the vertical distribution of concentration profile over time, which supports the hypothesis that groundwater elevation fluctuations correspond to a flux of nitrate-N.

Fig. 5 presents the simulated pressure head and nitrate-N concentration distribution at the bottom layer of the domain (between 8.99 and 9.48m below the ground surface based on surface topography) at six different time during 1993–1995. This layer was right at the bottom boundary of the modeling domain, and therefore, pressure head values were corresponding to the thickness of the groundwater in the domain. From October 1993 to October 1995, the groundwater thickness showed a trend of declining, with corresponding pressure head values ranged from 5.2 to 6.2m in Oct.1993, 4.5 to 5.5m in Oct. 1994, and 3.9 to 5m in Oct.1995. The pressure head was higher in the western part of the field than the eastern part, which resulted in a <1 m/year horizontal groundwater flow from northwest toward southeast.

At this layer, changing nitrate-N concentrations were also sensitive to changing groundwater levels. Nitrate-N concentrations were generally higher in the months with higher groundwater levels (Fig. 5). For example, nitrate-N concentrations were higher in April of 1994 and 1995 than October of 1994 and 1995, which was consistent with the observed higher pressure head in April of both years (Fig. 5). From April 1993 to October 1995, an overall decreasing trend in the nitrate-N concentration in the groundwater was observed, which can be attributed to the overall reduction of groundwater elevation in this period. In other words, a greater amount of nitrate-N mass left the domain and reduced the nitrate-N concentrations in the saturated part. **Fig. 6** presents the bottom layer water and solute flux over time. As clearly shown here, solute

Fig. 5. Distribution of the (a) pressure head (m) and (b) NO_3-N concentrations (mg L^{-1}) at the bottom layer of the domain (between 8.99 and 9.48m below the ground surface based on surface topography) on April 1st and October 1st of each year (1993 to 1995). April 1st of 1993 was used as initial condition for pressure head and nitrate-N concentration.

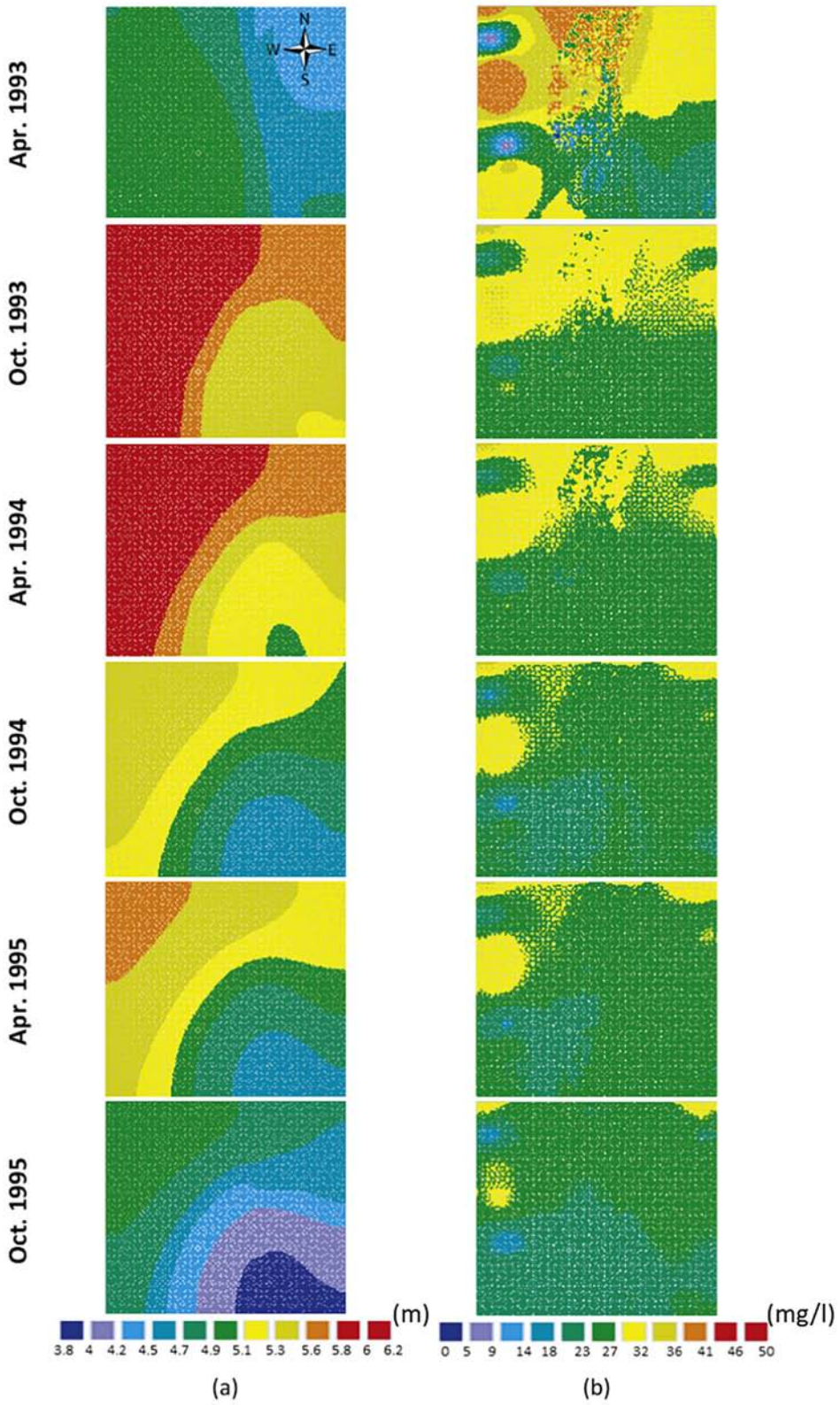
Apr. 1993
Oct. 1993
Apr. 1994
Oct. 1994
Apr. 1995
Oct. 1995
N
W
E
S
(m)
3.8 4 4.2 4.5 4.7 4.9 5.1 5.3 5.6 5.8 6 6.2
(a)
(mg/l)
0 5 9 14 18 23 27 32 36 41 46 50
(b)

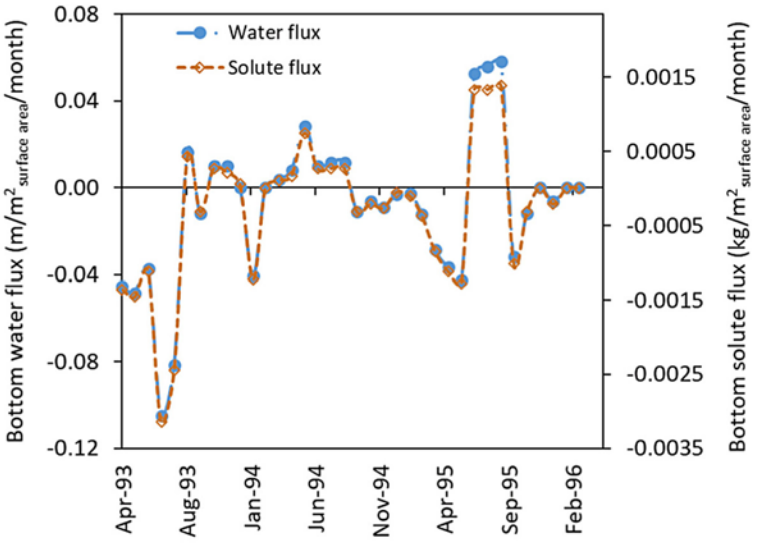

Fig. 6. Water flux (m/m² surface area/month) and nitrate-N mass flux (kg/m² surface area/month) at bottom of the domain. Positive flux means water/solute is removed from the system and negative flux means water/solute is added to the system.

flux variations closely followed the trend of groundwater flux, so that nitrate-N flux at the bottom was correspondent to the groundwater elevation fluctuation during the simulation period. This observation supports our hypothesis that the concentration of nitrate-N in the deeper part of the domain was correlated to the groundwater flux. This finding demonstrates the importance of coupling of the unsaturated-zone and saturated-zone in investigating nitrate-N transport in the subsurface.

4.3. Impacts of soil heterogeneity on the nitrate-N in the domain

As shown in **Fig. 7,** four different types of loam were distributed in the top 3m of the simulation domain. Below 3 m, the domain was homogeneously composed of sandy loam. To evaluate the impacts of soil heterogeneity in the first 3m of the domain, a same simulation was conducted in a homogeneous domain composed of only sandy loam across the whole domain. Fig. 8 highlights a comparison of pressure head and nitrate-N concentration between homogeneous and heterogeneous domain on Oct. 1st of 1995 at the depth of 2m from the ground surface.

In the homogenous domain, water pressure head was higher in the eastern part of the domain than the western part despite the identical soil properties everywhere, which was due to uneven surface topography

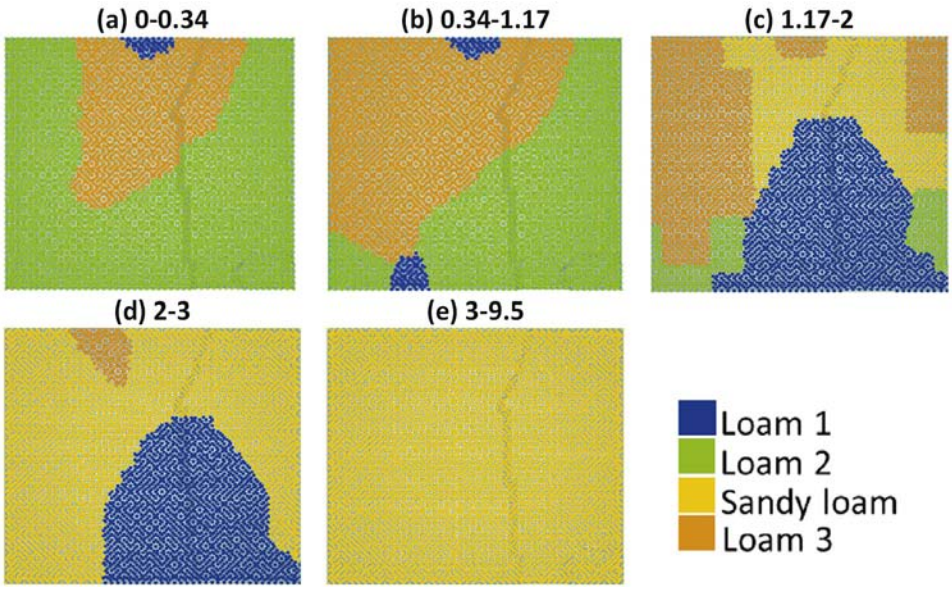

Fig. 7. Sediment type representing soil heterogeneity at different soil depth intervals (m).

where surface elevation in the eastern part was about 0.5m lower than in the western part. The minimum (in the west) and maximum (in the east) water content were about 0.18 and 0.21 in the homogenous domain and 0.11 and 0.31 in the heterogeneous domain, respectively. Moreover, the pressure head distribution in the homogenous soil domain was uniform. For the heterogeneous domain (Fig. 8), the spatial distribution of pressure head was correlated to the sediment distribution (Fig. 7). Particularly, loam 1 delineated a zone with varying soil moisture content in the heterogeneous domain with relatively lower pressure head (ca. −4.8 to −3.2 m) in the western part of the domain than the adjacent area (ca. −2.6 to −2.1 m). According to the soil particle size analysis (Table 1), soil samples from loam 1, loam 2, and loam 3 have different hydraulic parameters although they all belong to general loam category. Loam 1 was majorly located between 1.17m and 3m from the surface, and because the water holding capacity of loam 1 was higher than the sandy loam in the surrounding area, water infiltration rate above loam 1 was reduced, which led to a decreased water pressure head at the 2m layer.

Similar to the pressure head distributions, the nitrate-N distribution at the 2m soil layer was also impacted by the soil heterogeneity and surface topography (Fig. 8b). Due to the lower surface elevation in the eastern part of the domain, nitrate-N reached this level more rapidly,

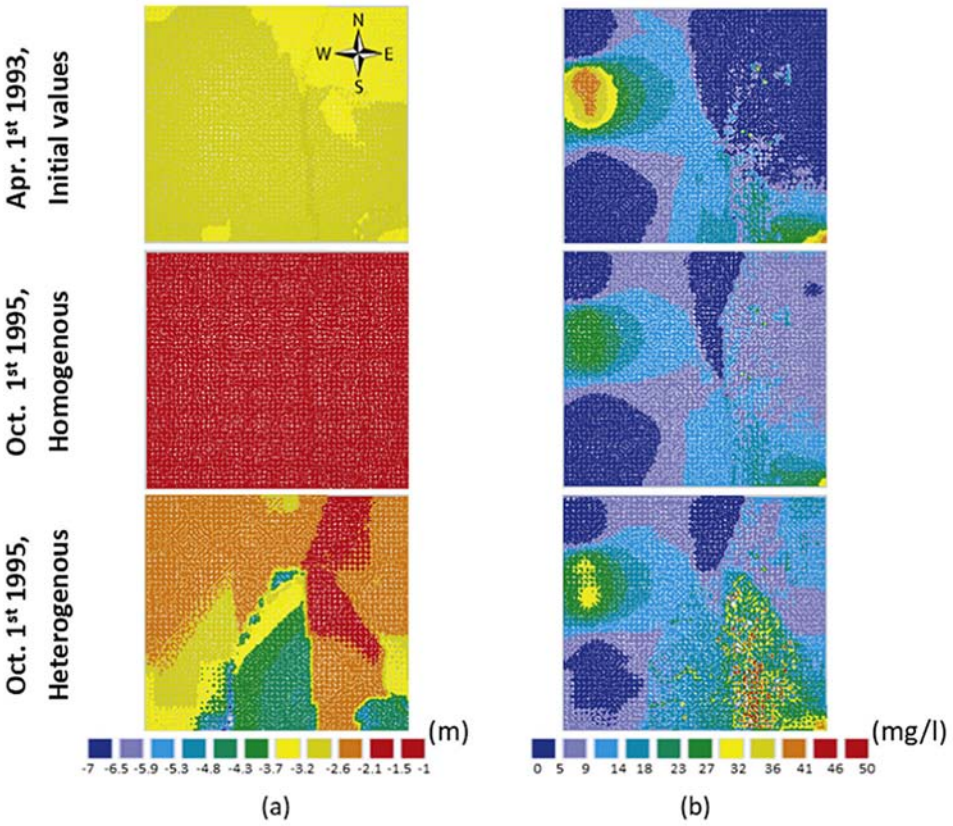

Fig. 8. Distribution of the (a) pressure head (m) and (b) NO_3-N concentrations (mg L^{-1}) at 2m below the ground surface on April 1st, 1993 and October 1st, 1995 for the homogenous and heterogeneous soil domains. Values of pressure head and nitrate-N concentration on April 1st of 1993 were used as initial conditions for both homogenous and heterogeneous soil domains.

therefore higher nitrate-N concentration was observed in the eastern part. Point-by-point comparisons showed that nitrate-N concentrations in the homogenous domain were either equal to or lower than that in the heterogeneous domain (Fig. 8b), with the same surface loading and simulation duration. Higher nitrate-N concentration in the heterogeneous domain could be partially attributed to the drier soil condition at the 2m soil layer (Fig. 8a), because the higher soil moisture content in the homogenous soil layer could result in the dilution of nitrate-N and reduced concentration. In addition, less nitrate-N was retained in this layer in the homogenous domain due to the promoted infiltration within the sandy loam soil type. In the heterogeneous domain, nitrate-N infiltration rates from high to low followed the order of Sandy loam > Loam 1 > Loam 2 > Loam 3, which was the same order for the soil saturated

hydraulic conductivity and inversely related to residual water content. Higher hydraulic conductivity and lower soil water holding capacity will lead to higher water flux in the soil and correspondingly increased the nitrate-N infiltration. Assuming a homogenous soil domain composed of sandy loam everywhere, the leaching rate of nitrate-N was higher across the domain compared to the heterogeneous domain and lower concentration of nitrate-N was observed at 2m from top. This observation is consistent with a previous work (Russo et al., 2013), where the modeling results demonstrate that a heterogeneous model with realistic distribution of soil properties is necessary to provide the spatial variability of nitrate-N in the field. Overall, the total amount of nitrate-N mass was not significantly different in the heterogeneous and homogeneous domains during the simulation period. In another study (Botros et al., 2012), nitrate-N transport in a 3-D domain was simulated by considering various level of heterogeneities, all models resulted in very similar nitrate mass in the deep vadose zone. The minimal impact of heterogeneity on the total mass of nitrate-N in the domain was attributed to the repeated irrigation and fertilizer application, which could also be the case for this study site.

5. Conclusion

We investigated nitrate-N transport in a field site by integrating 3-D numerical modeling with comprehensive field measurements. The work was based on a data dense site in Nebraska, where the shallow groundwater beneath was contaminated with nitrate-N concentration (about 32 mg L^{-1}) primarily as a result of nitrate-N leaching from the root zone of Nebraska's two million hectares of irrigated corn fields (Klocke et al., 1999). Here, a realistic 3-D lithology model was first developed based on comprehensive well log information in the Nebraska MESA site. A 3-D hydrological model was then developed to simulate water flow and nitrate-N transport in the site. In parallel, a homogeneous soil domain, containing the major sediment type of the site (i.e. sandy loam), was developed to compare the water flow and nitrate-N leaching in both domains.

In this work, the 3-D soil and vadose zone lithology profile represented an unsaturated subsurface media combined with a saturated zone at the bottom. Short-term variations of nitrate-N concentration at the bottom of the domain (in the saturated part) are correlated to

groundwater elevation fluctuations. When groundwater level rose, greater mass of nitrate-N was added to the system and consequently increased the nitrate-N concentration. This work highlights the importance of considering groundwater level changes in simulating nitrate-N concentration in the deeper vadose zone.

The soil heterogeneity on the site was mainly observed at the top soil down to 3m from the surface, and deeper parts were relatively homogeneous aquifer matrix. Heterogeneous soil properties has comprehensively impacted the spatial distribution of nitrate-N concentration. 3-D modeling was helpful to visualize spatial variations of nitrate- N concentration at different screening depths and relate this variability to sediments distribution. Sediment types with higher saturated hydraulic conductivity and lower residual water content had lower water holding capacity which increased water infiltration rate as well as nitrate-N leaching rates. Soil heterogeneity, however, has minimal impact on the total mass of nitrate-N in the domain.

Acknowledgment — This research was supported by a project entitled "Influence of Climate and Agricultural Clustering on Groundwater Contamination by Trace Organics," which was sponsored by the United States Department of Agriculture Grant No. 2014-67003-22072. We would also like to thank the MSEA site cooperators for their assistance in collection of additional samples from their fields, as well as extensive assistance from previous Nebraska MSEA site investigators.

References

AmeriFlux Site, Data Exploration System, 2016. Available at. http://ameriflux.ornl.gov/

Arbat, G., Roselló, A., Olivé, F.D., Puig-Bargués, J., Llinàs, E.G., Duran-Ros, M., Pujol, J., De Cartagena, F.R., 2013. Soil water and nitrate distribution under drip irrigated corn receiving pig slurry. Agric. Water Manag. 120, 11–22.

Baram, S., Couvreur, V., Harter, T., Read, M., Brown, P.H., Kandelous, M., Smart, D.R., Hopmans, J.W., 2017. Estimating nitrate leaching to groundwater from Orchards: comparing crop nitrogen excess, deep vadose zone data-driven estimates, and HYDRUS modeling. Vadose Zo. J. 15 (11), 1–13.

Botros, F.E., Onsoy, Y.S., Ginn, T.R., Harter, T., 2012. Richards equation-based modeling to estimate flow and nitrate transport in a deep alluvial vadose zone. Vadose Zo. J. 11 (4) Available at https://dl.sciencesocieties.org/publications/vzj/pdfs/11/4/vzj2011.0145

Cabon, F., Girard, G., Ledoux, E., 1991. Modelling of the nitrogen cycle in farm land areas. Fertil. Res. 27 (2–3), 161–169.

Chaudhuri, S., Ale, S., 2014. Long term (1960–2010) trends in groundwater contamination and salinization in the Ogallala aquifer in Texas. J. Hydrol. 513, 376–390.

Deb, S.K., Sharma, P., Shukla, M.K., Ashigh, J., Šimůnek, J., 2015. Numerical evaluation of nitrate distributions in the onion root zone under conventional furrow fertigation. J. Hydrol. Eng. 21 (2), 5015026.

Exner, M.E., Spalding, R.F., 1990. Occurrence of Pesticides and Nitrate in Nebraska's Ground Water. Lincoln, NE.

Feddes, R.A., Kowalik, P.J., Zaradny, H., 1978. Simulation of Field Water Use and Crop Yield. John Wiley & Sons, New York, NY.

Gärdenäs, A.I., Hopmans, J.W., Hanson, B.R., Šimůnek, J., 2005. Two-dimensional modeling of nitrate leaching for various fertigation scenarios under micro-irrigation. Agric. Water Manag. 74 (3), 219–242.

Hanson, B.R., Šimůnek, J., Hopmans, J.W., 2006. Evaluation of urea-ammonium-nitrate fertigation with drip irrigation using numerical modeling. Agric. Water Manag. 86 (1), 102–113.

Hassan, G., Reneau, R.B., Hagedorn, C., Jantrania, A.R., 2008. Modeling effluent distribution and nitrate transport through an on-site wastewater system. J. Environ. Qual. 37 (5), 1937–1948. Available at https://www.agronomy.org/publications/jeq/abstracts/37/5/1937

High Plains Regional Climate Center, 2016. Available at http://www.hprcc.unl.edu/

Hu, K., Li, B., Chen, D., Zhang, Y., Edis, R., 2008. Simulation of nitrate leaching under irrigated maize on sandy soil in desert oasis in Inner Mongolia, China. Agric. Water Manag. 95 (10), 1180–1188.

Ippisch, O., Vogel, H.J., Bastian, P., 2006. Validity limits for the van Genuchten–Mualem model and implications for parameter estimation and numerical simulation. Adv. Water Resour. 29 (12), 1780–1789.

Iqbal, S., Guber, A.K., Khan, H.Z., 2016. Estimating nitrogen leaching losses after compost application in furrow irrigated soils of Pakistan using HYDRUS-2D software. Agric. Water Manag. 168, 85–95.

Jansson, P.E., Karlberg, L., 2010. Coupled Heat and Mass Transfer Model for Soil-Plant-Atmosphere Systems. Stockholm.

Keating, B.A., Carberry, P.S., Hammer, G.L., Probert, M.E., Robertson, M.J., Holzworth, D., Huth, N.I., Hargreaves, J.N., Meinke, H., Hochman, Z., McLean, G., 2003. An overview of APSIM, a model designed for farming systems simulation. Eur. J. Agron. 18 (3), 267–288.

Klocke, N.L., Watts, D.G., Schneekloth, J.P., Davison, D.R., Todd, R.W., Parkhurst, A.M., 1999. Nitrate leaching in irrigated corn and soybean in a semi-arid climate. Trans. ASAE 42 (6), 1621–1630.

Lasserre, F., Razack, M., Banton, O., 1999. A GIS-linked model for the assessment of nitrate contamination in groundwater. J. Hydrol. 224 (3), 81–90.

Ledoux, E., Gomez, E., Monget, J.M., Viavattene, C., Viennot, P., Ducharne, A., Benoît, M., Mignolet, C., Schott, C., Mary, B., 2007. Agriculture and groundwater nitrate contamination in the Seine basin. The STICS-MODCOU modelling chain. Sci. Total Environ. 375 (1), 33–47.

Lee, M.S., Lee, K.K., Hyun, Y., Clement, T.P., Hamilton, D., 2006. Nitrogen transformation and transport modeling in groundwater aquifers. Ecol. Model. 192 (1), 143–159.

Ling, G., El-Kadi, A.I., 1998. A lumped parameter model for nitrogen transformation in the unsaturated zone. Water Resour. Res. 34 (2), 203–212.

Lotse, E.G., Jabro, J.D., Simmons, K.E., Baker, D.E., 1992. Simulation of nitrogen dynamics and leaching from arable soils. J. Contam. Hydrol. 10 (3), 183–196.

Ma, L., Scott, H.D., Shaffer, M.J., Ahuja, L.R., 1998. RZWQM simulations of water and nitrate movement in a manured tall fescue field. Soil Sci. 163 (4), 259–270.

MacQuarrie, K.T.B., Sudicky, E.A., Robertson, W.D., 2001. Numerical simulation of a fine-grained denitrification layer for removing septic system nitrate from shallow groundwater. J. Contam. Hydrol. 52 (1), 29–55.

Martin, G.E., Snow, D.D., Kim, E., Spalding, R.F., 1995. Simultaneous determination of argon and nitrogen. Ground Water 33 (5), 781–785. Available at https://doi.org/10.1111/j.1745-6584.1995.tb00024.x

Mcguire, V.L., Kilpatrick, J.M., 1998. Hydrogeology in the Vicinity of the Nebraska Management Systems Evaluation Area Site, Central Nebraska.

McMahon, P.B., Dennehy, K.F., Bruce, B.W., Böhlke, J.K., Michel, R.L., Gurdak, J.J., Hurlbut, D.B., 2006. Storage and transit time of chemicals in thick unsaturated zones under rangeland and irrigated cropland, High Plains, United States. Water Resour. Res. 42 (3) Available at https://doi.org/10.1029/2005WR004417

Misra, C., Nielsen, D.R., Biggar, J.W., 1974. Nitrogen transformations in soil during leaching; I. Theoretical considerations. Soil Sci. Soc. Am. J. 38 (2), 289–293.

Mitsch, W.J., Day, J.W., 2006. Restoration of wetlands in the Mississippi-Ohio-Missouri (MOM) river basin: experience and needed research. Ecol. Eng. 26 (1), 55–69.

Mualem, Y., 1976. A new model for predicting the hydraulic conductivity of unsaturated porous media. Water Resour. Res. 12 (3), 513–522. Available at https://doi.org/10.1029/WR012i003p00513

Nakamura, K., Harter, T., Hirono, Y., Horino, H., Mitsuno, T., 2004. Assessment of root zone nitrogen leaching as affected by irrigation and nutrient management practices. Vadose Zo. J. 3 (4), 1353–1366.

Neuman, S.P., 1990. Universal scaling of hydraulic conductivities and dispersivities in geologic media. Water Resour. Res. 26 (8), 1749–1758.

Nitrogen Efficiency, 2016. Available at https://www.nachurs.com

Plaza-bonilla, D., Nolot, J., Raffaillac, D., Justes, E., 2015. Cover crops mitigate nitrate leaching in cropping systems including grain legumes: field evidence and model simulations. Agric. Ecosyst. Environ. 212, 1–12. Available at https://doi.org/10.1016/j.agee.2015.06.014

Poch-Massegú, J.R., Jiménez-Martínez, K.J. Wallis, de Cartagena, F.R., Candela, L., 2014. Irrigation return flow and nitrate leaching under different crops and irrigation methods in Western Mediterranean weather conditions. Agric. Water Manag. 134, 1–13.

Ramos, T.B., Šimůnek, J., Gonçalves, M.C., Martins, J.C., Prazeres, A., Pereira, L.S., 2012. Two-dimensional modeling of water and nitrogen fate from sweet sorghum irrigated with fresh and blended saline waters. Agric. Water Manag. 111, 87–104.

RockWare, Inc, 2016. Available at https://www.rockware.com/

Russo, D., Zaidel, J., Laufer, A., 2001. Numerical analysis of flow and transport in a combined heterogeneous vadose zone - groundwater system. Adv. Water Resour. 24 (1), 49–62.

Russo, D., Laufer, A., Shapira, R.H., Kurtzman, D., 2013. Assessment of solute fluxes beneath an orchard irrigated with treated sewage water: a numerical study. Water Resour. Res. 49 (2), 657–674.

Schaap, M.G., Leij, F.J., Van Genuchten, M.T., 2001. Rosetta: a computer program for estimating soil hydraulic parameters with hierarchical pedotransfer functions. J. Hydrol. 251 (3), 163–176.

Schepers, J.S., G.E. Varvel, and D.G. Watts. 1995. Nitrogen and water management strategies to reduce nitrate leaching under irrigated maize. 20(3): 227–239.

Selim, H.M., Iskandar, I.K., 1981. Modeling nitrogen transport and transformations in soils: 2. Validation. Soil Sci. 131 (5), 303–312.

Šimůnek, J., van Genuchten, M.T., Šejna, M., 2016. Recent developments and applications of the HYDRUS computer software packages. Vadose Zo. J. 15 (7).

Skaggs, T.H., Trout, T.J., Šimůnek, J., Shouse, P.J., 2004. Comparison of HYDRUS-2D simulations of drip irrigation with experimental observations. J. Irrig. Drain. Eng. 130 (4), 304–310.

Soil and Health Library, 2016. Available at https://www.soilandhealth.org

Spalding, R.F., Exner, M.E., 1993. Occurrence of nitrate in groundwater—a review. J. Environ. Qual. 22 (3), 392–402.

Spalding, R.F., Watts, D.G., Schepers, J.S., Burbach, M.E., Exner, M.E., Poreda, R.J., Martin, G.E., 2001. Controlling nitrate leaching in irrigated agriculture. J. Environ. Qual. 30 (4), 1184–1194.

Stigter, T.Y., Carvalho Dill, A.M.M., Ribeiro, L., 2011. Major issues regarding the efficiency of monitoring programs for nitrate contaminated groundwater. Environ. Sci. Technol. 45 (20), 8674–8682.

Stöckle, C.O., Donatelli, M., Nelson, R., 2003. CropSyst, a cropping systems simulation model. Eur. J. Agron. 18 (3), 289–307.

Tafteh, A., Sepaskhah, A.R., 2012. Application of HYDRUS-1D model for simulating water and nitrate leaching from continuous and alternate furrow irrigated rapeseed and maize fields. Agric. Water Manag. 113, 19–29.

Tillotson, W.R., 1980. Soil Water, Solute and Plant Growth Simulation. University of Nebraska–Lincoln, N-L, 2000. Quality-Assessed Agrichemical Contaminant Database for Nebraska Ground Water. Available at http://nednr.nebraska.gov/Clearinghouse/Clearinghouse.aspx

van der Laan, M., Annandale, J.G., Bristow, K.L., Stirzaker, R.J., Du Preez, C.C., Thorburn, P.J., 2014. Modelling nitrogen leaching: are we getting the right answer for the right reason? Agric. Water Manag. 133, 74–80.

Van Genuchten, M.T., 1980. A closed-form equation for predicting the hydraulic conductivity of unsaturated soils 1. Soil Sci. Soc. Am. J. 44 (5), 892–898.

Wang, Z., Li, J., Li, Y., 2014. Simulation of nitrate leaching under varying drip system uniformities and precipitation patterns during the growing season of maize in the North China plain. Agric. Water Manag. 142, 19–28.

Water Research Center, 2014. Available at http://www.water-research.net/

Zhu, A., Zhang, J., Zhao, B., Cheng, Z., Li, L., 2005. Water balance and nitrate leaching losses under intensive crop production with Ochric Aquic Cambosols in North China Plain. Environ. Int. 31 (6), 904–912.